Electronic Supplementary Material (ESI) for New Journal of Chemistry.

Organo-metallic electrolyte additives for regulating hydrogen evolution and self-discharge in Mg-air aqueous batteries

Kandeeban Rajagopalan[a], Brindha Ramasubramanian[b], Manojkumar Kaliannan[a], Seeram Ramakrishna[b], P. Marappan[c], Ramasamy Kulandaivel Saminathan*[a]

[a.] *Department of chemistry, Kongunadu arts and science college, G.N. Mills, Coimbatore, Tamil Nadu – 641029, India. E-mail: ksaminath@gmail.com*
[b.] *Center for Nanofibers and Nanotechnology, Department of Mechanical Engineering, National University of Singapore, Singapore 117574, Singapore.*
[c.] *SAM Technologies, Coimbatore – 641029, India*

Table s1 Corrosion inhibition over elevated temperatures

Temp / Conc of Inhibitor	303 K		313 K		323 K		333 K	
	CR X 10^{-2} (mmpy)	IE%	CR X 10^{-2} (mmpy)	IE %	CR X 10^{-2} (mmpy)	IE %	CR X 10^{-2} (mmpy)	IE %
0	127.04		140.46		147.36		155.32	
200	49.72	59.95	81.72	41.46	96.52	34.19	110.3	28.83
300	38.54	69.85	75.94	45.83	89.26	39.47	103.51	33.15
400	30.44	75.79	69.38	50.74	81.07	44.64	96.65	37.91
500	15.54	87.79	63.63	54.47	74.92	49.16	90.26	41.64
600	12.62	89.46	46.49	66.61	65.54	55.40	84.32	45.66
700	12.93	89.23	48.92	65.61	66.46	54.76	84.76	44.82
800	13.41	89.03	48.54	65.35	67.44	54.14	87.49	43.51

Table s2 Isotherm parameters with varying temperature and concentrations

Inhibitor concentration (g/L) X 10^{-1}	Surface coverage (θ) X10^{-2}				C/θ X10^{2}			
	303 K	313 K	323 K	333 K	303 K	313 K	323 K	333 K
0.2	0.5995	0.4146	0.3419	0.2883	0.33361134	0.482393	0.58496636	0.693722
0.3	0.6985	0.4584	0.3947	0.3315	0.42949177	0.65445	0.76007094	0.904977
0.4	0.7579	0.5074	0.4187	0.3791	0.52777411	0.788333	0.95533795	1.055131
0.5	0.8394	0.5732	0.4662	0.4164	0.59566357	0.872296	1.07250107	1.200768
0.6	0.91	0.65	0.5317	0.4566	0.65934066	0.923077	1.1284559	1.31406
0.7	0.9124	0.6651	0.5535	0.474	0.76720737	1.052473	1.26467931	1.476793
0.8	0.9125	0.6794	0.5857	0.4802	0.87671233	1.17751	1.36588697	1.665973

Table s3 Potentiodynamic polarization measurements

Parameters (g) X 10^{-1}	I_{corr} (μA)	$-E_{corr}$ (V)	Linear polarization (ohm)	Cathode slope (mV dec^{-1})	Anode slope (mV dec^{-1})	Corrosion rate (mil/year) e-1	Inhibition efficiency (%)
Plain	157.4	1.49	47991	5.839	4.903	5.760	
2	72.6	1.45	42486	4.946	5.011	2.046	64.47917
4	44.1	1.43	39489	5.110	5.061	1.213	78.94097
6	21.1	1.43	38826	5.140	5.004	0.538	90.65972
8	31.8	1.43	48923	4.792	4.810	1.476	74.375

Table s4 Comparison with previous works regarding corrosion inhibitor

S. no.	Material	Inhibitor	Concentration of Inhibitor	Electrolyte	Efficiency	References
1.	AZ91D	walnut green husk extract	1.0 g L^{-1}	NaCl	92.5 %	[1]
2.	AM50	3-amino-1,2,4-triazole-5-thiol (ATT) and NaF	50 mM NaF : 5 mM ATT	NaCl	95.8%	[2]
3.	AZ31B	benzyl triphenyl phosphonium bis(trifluoromethylsulfonyl) amide	0.30 mM	NaCl	91.4%	[3]
4.	AZ31	sodium molybdate	150 mM	NaCl	78%	[4]
5.	AZ31	Hexamethyl cyclotrisiloxane	600 ppm	NaCl	92%	This work

Table s5 Comparison with previous works regarding corrosion inhibitor in Mg-Air Battery

S. no.	Material	Inhibitor	Concentration of Inhibitor	Electrolyte	Efficiency	References
1.	Pure Mg	Complexing agent	0.05 M	NaCl	Improvement of 210 mV during discharge	[5]
2.	AZ91	Sodium Phosphate	0.5 g · L^{-1}	NaCl	discharge potential increases from 1.120 V to 1.150 V	[6]
3.	AZ91	Sodium Dodecylbenzenesulfonate	0.5 g · L^{-1}	NaCl	inhibition efficiency can reach 95.2%	[6]
4.	Pure Mg	Decyl glucoside	4.5 mM	NaCl	Inhibition efficiency 94%	[7]
5.	AZ31	Hexamethyl cyclotrisiloxane	600 ppm	NaCl	Inhibition efficiency 92%, with an anodic utilization efficiency of 60.08%	This work

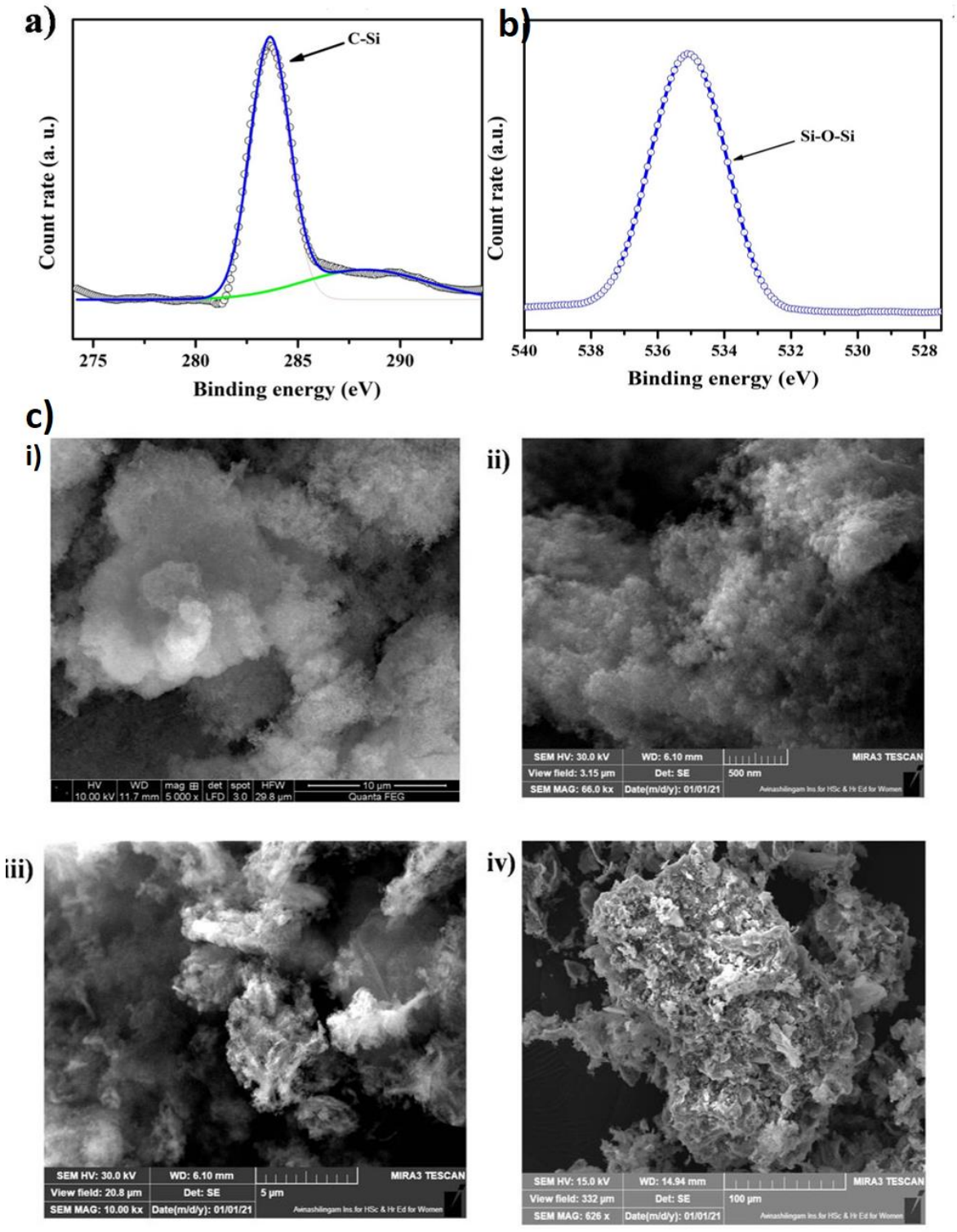

Figure s1: a,b) XPS spectra of D3, c) SEM of synthesized D3

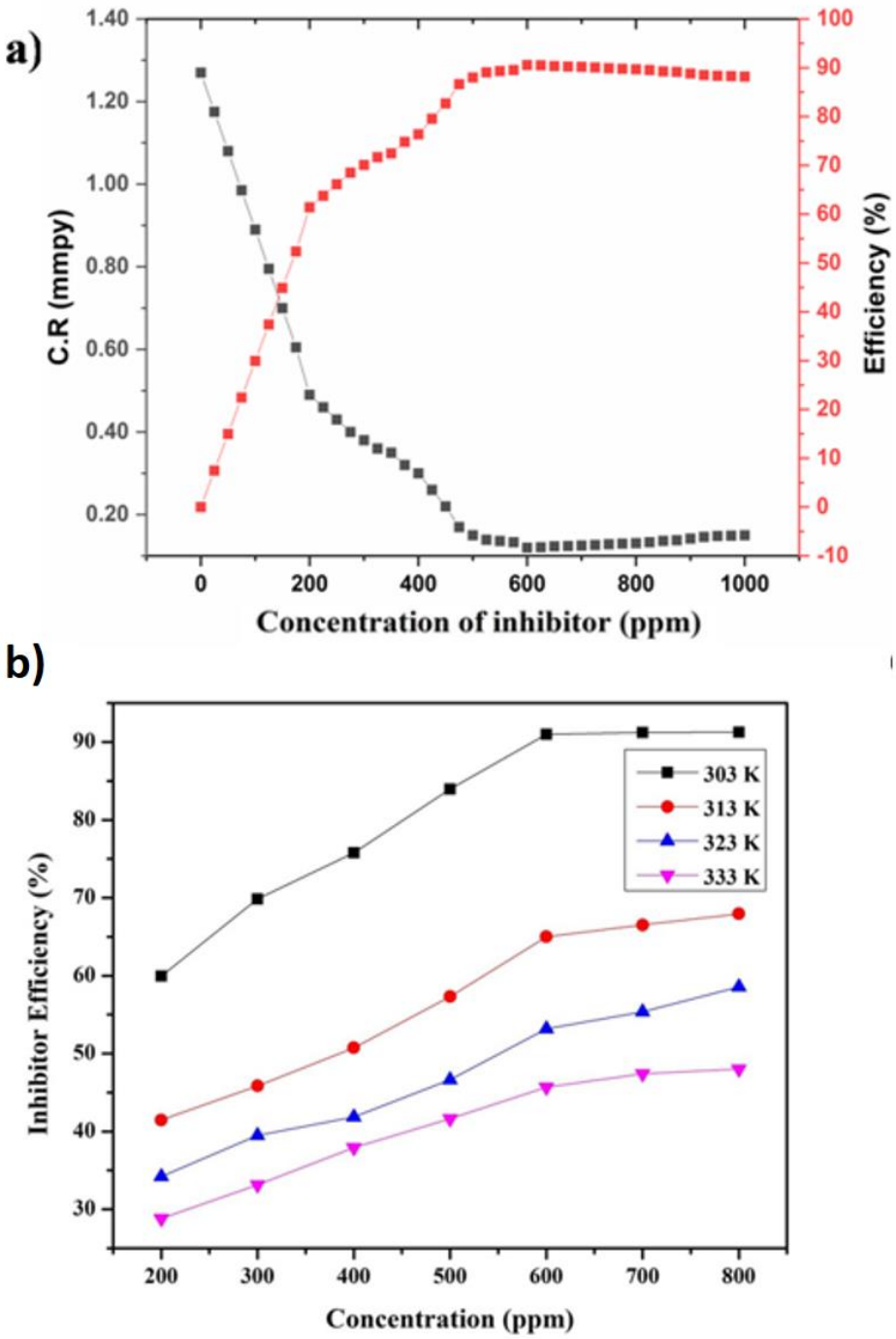

Figure s2: a) Corrosion rate and Efficiency over various concentration protected Mg alloy, b) Inhibitor efficiency over various concentrations at elevated temperatures

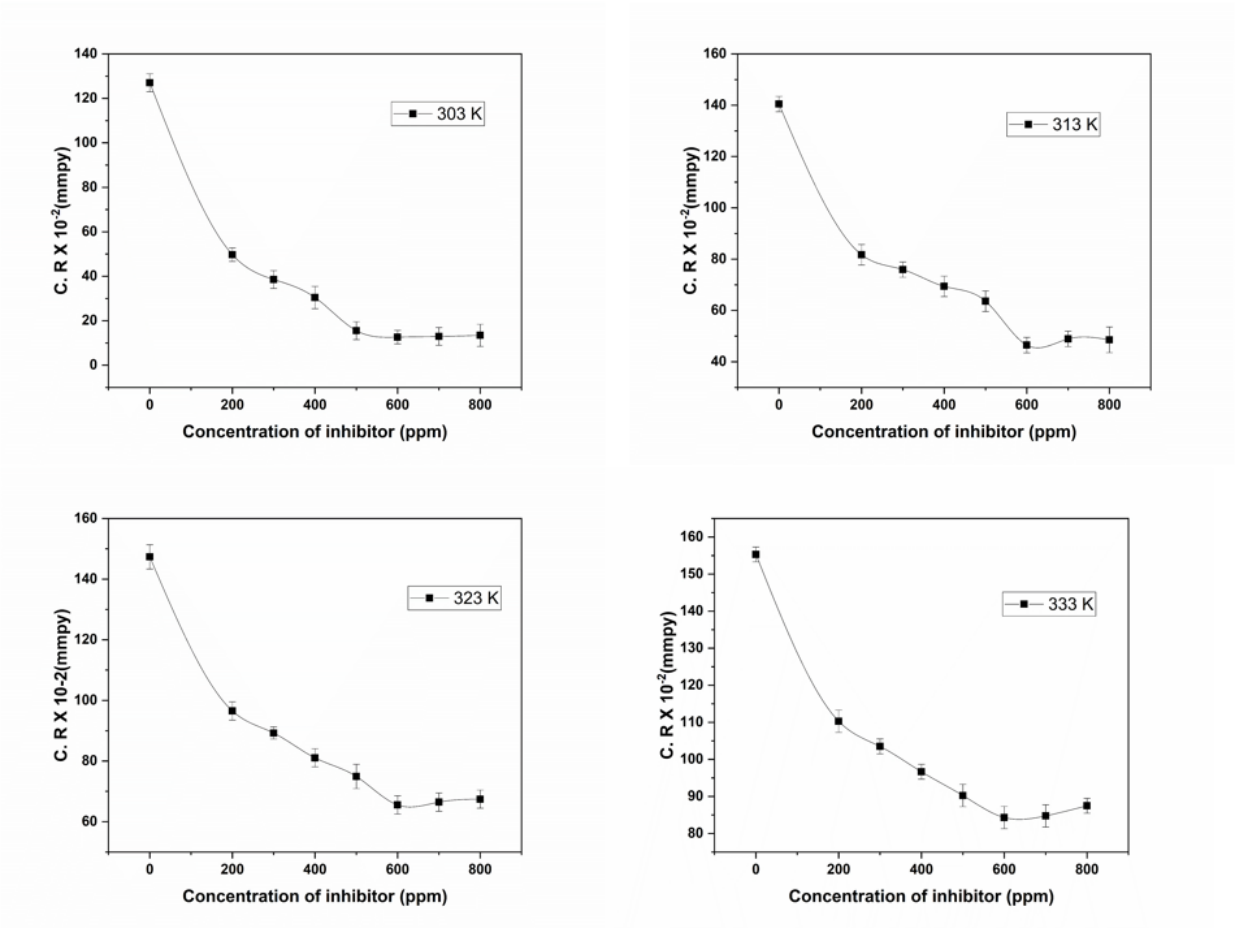

Figure s3: The standard deviation error bar marked values of corrosion rate over different concentration of inhibitor at a) 303K, b) 313 K, c) 323 K, d) 333 K

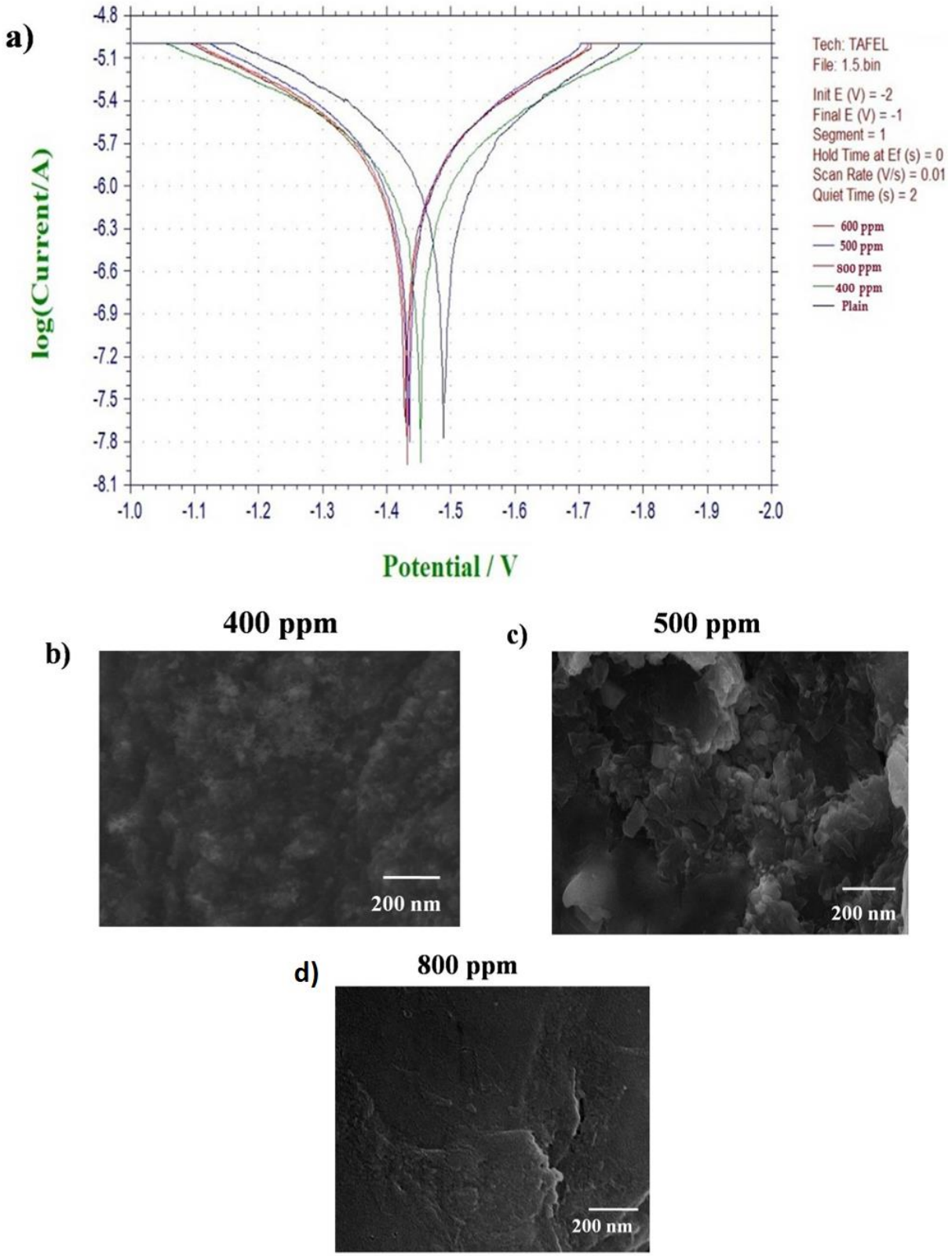

Figure s4: a) Potentiodynamic polarization of Mg with and without D3, b-d) different concentration of D3 inhibitor protected Mg alloy

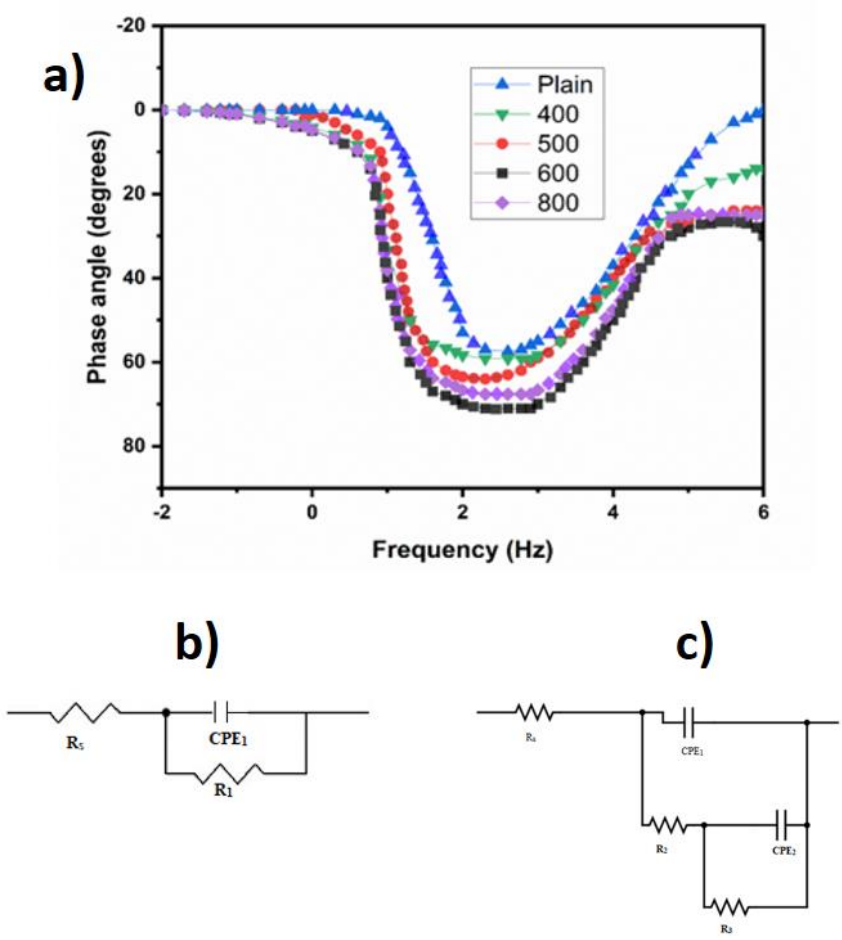

Figure s5: a) Bode-phase plot, b) circuit fitted for plain corrosive medium, c) Circuit fitted for inhibitor added medium

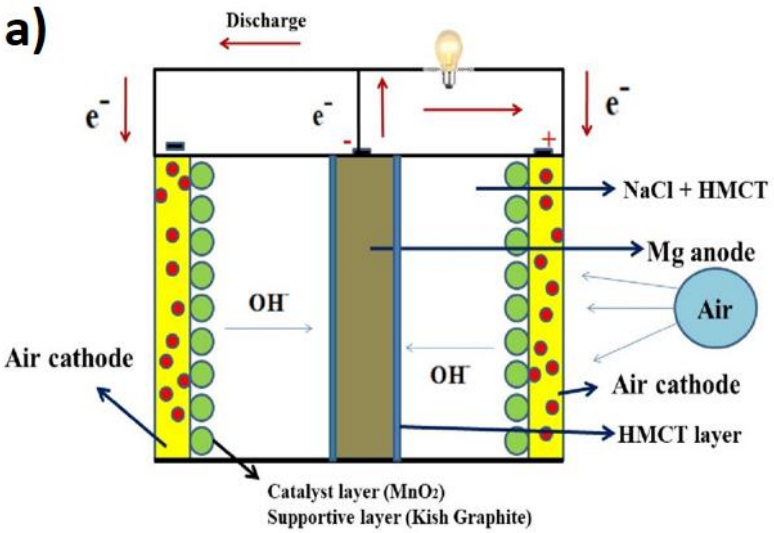

Figure s6: a) Design of fabricated cell system

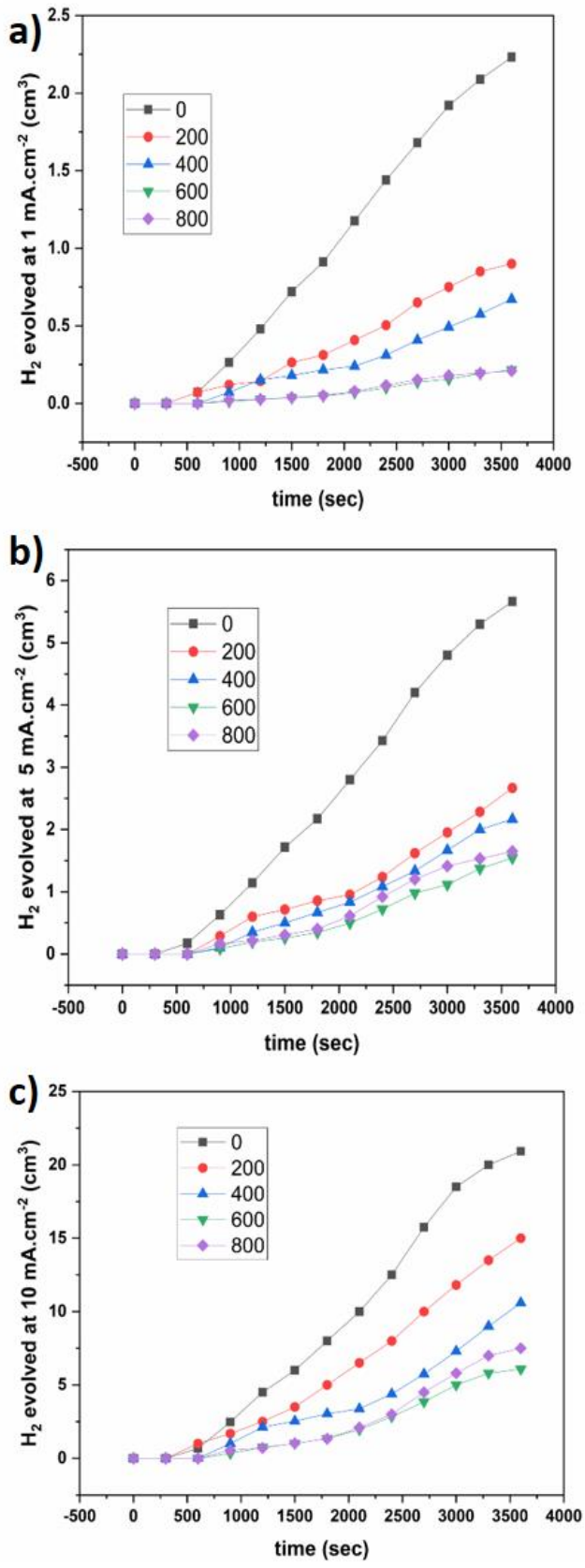

Figure s7: Hydrogen evolution of D3 protected Mg-air battery at a) 1 mA. cm^{-2} b) 5 mA. cm^{-2} c) 10 mA. cm^{-2}

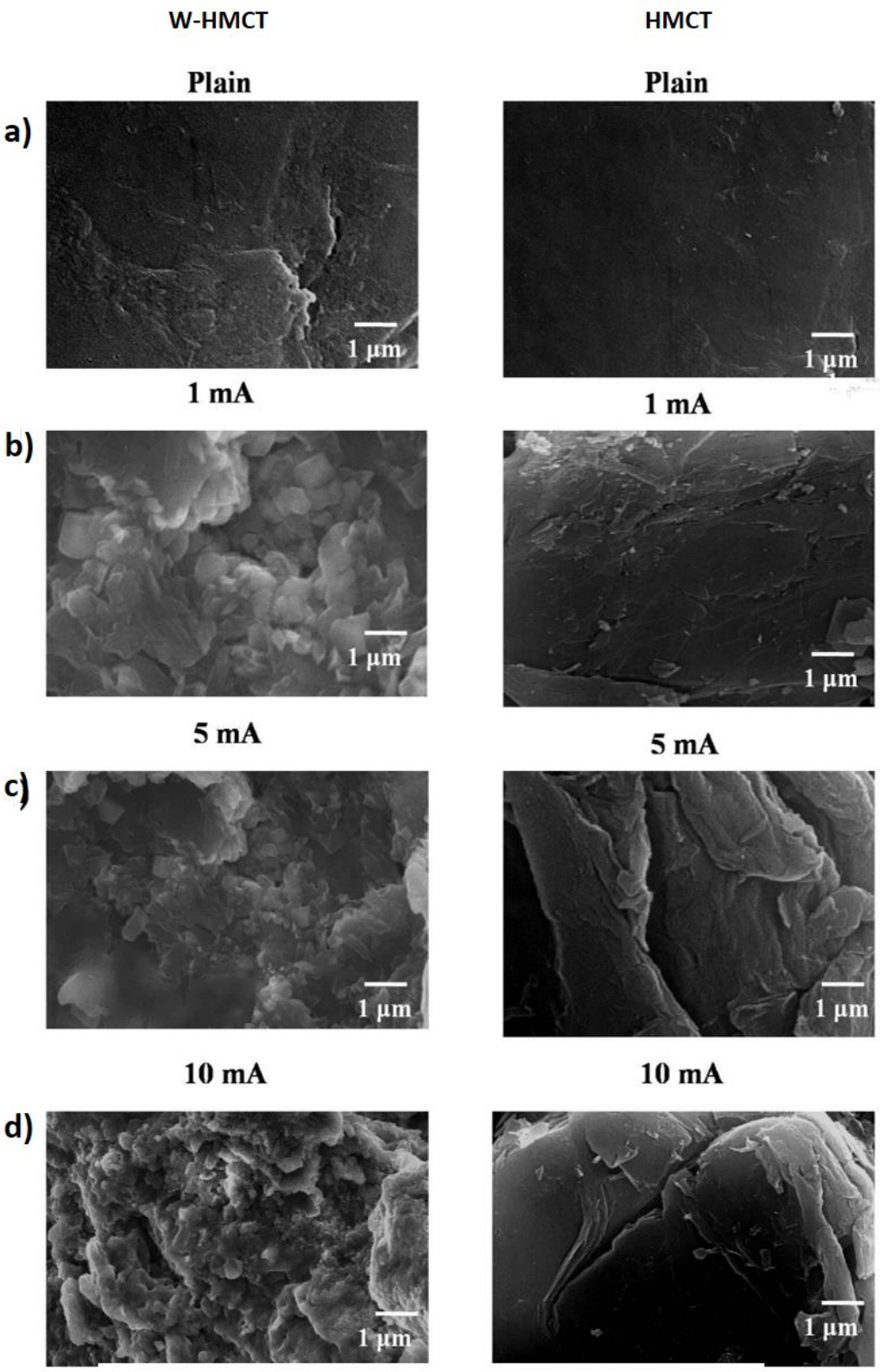

Figure s8: AFM images of anode Mg alloy after battery discharge at different current densities

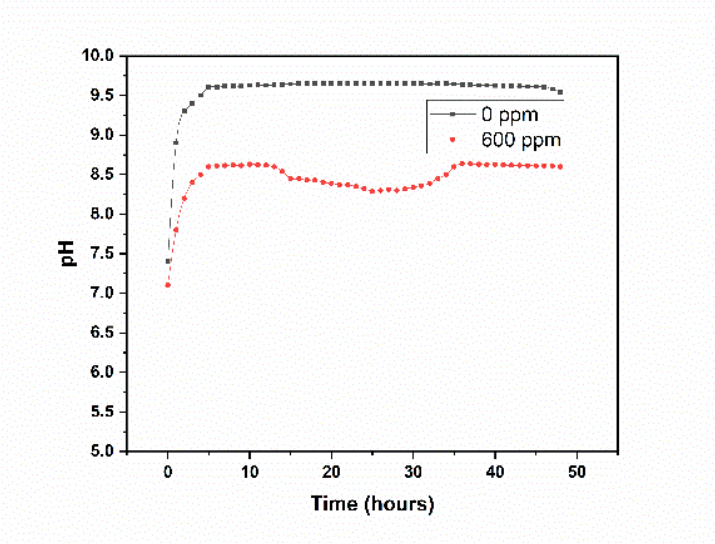

Figure s9: pH of the electrolyte with and without inhibitor during discharge

References:

1 Y. Wu, Y. Zhang, Y. Jiang, N. Li, Y. Zhang, L. Wang and J. Zhang, *Colloids Surfaces A Physicochem. Eng. Asp.*, 2021, **626**, 126969.

2 D. Huang, J. Tao, M. Cheng, R. Deng, S. Chen, L. Yin and R. Li, *J. Hazard. Mater.*, 2020, 124399.

3 H. Su, Y. Liu, X. Gao, Y. Qian, W. Li, T. Ren, L. Wang and J. Zhang, *Corrosion inhibition of magnesium alloy in NaCl solution by ionic liquid: Synthesis, electrochemical and theoretical studies*, Elsevier B.V., 2019, vol. 791.

4 M. A. Osipenko, D. S. Kharytonau, A. A. Kasach, J. Ryl, J. Adamiec and I. I. Kurilo, *Electrochim. Acta*, 2022, **414**, 140175.

5 B. Vaghefinazari, D. Höche, S. V. Lamaka, D. Snihirova and M. L. Zheludkevich, *J. Power Sources*, , DOI:10.1016/j.jpowsour.2020.227880.

6 Y. Li, J. Ma, G. Wang, F. Ren, Y. Zhu and Y. Song, *J. Electrochem. Soc.*, 2018, **165**, A1713–A1717.

7 M. A. Deyab, *J. Power Sources*, 2016, **325**, 98–103.